REPORT DOCUMENTATION PAGE

Form Approved OMB NO. 0704-0188

1. REPORT DATE (DD-MM-YYYY)	2. REPORT TYPE	3. DATES COVERED (From - To)
16-07-2008	New Reprint	1-Jan-2007 - 31-Dec-2007

4. TITLE AND SUBTITLE	5a. CONTRACT NUMBER
Epitaxially grown colloidal crystals of silica microspheres on patterned substrate of triangular arrays, Materials Science and Engineering C, 27, 961–967 (2007).	DAAD19-03-1-0227
	5b. GRANT NUMBER
	5c. PROGRAM ELEMENT NUMBER 611103

6. AUTHORS	5d. PROJECT NUMBER
Wonmok Lee and Paul V. Braun	
	5e. TASK NUMBER
	5f. WORK UNIT NUMBER

7. PERFORMING ORGANIZATION NAMES AND ADDRESSES	8. PERFORMING ORGANIZATION REPORT NUMBER
University of Illinois - Urbana - Champaign Office of Sponsored Programs 1901 S. First Street Champaign, IL 61820 -	

9. SPONSORING/MONITORING AGENCY NAME(S) AND ADDRESS(ES)	10. SPONSOR/MONITOR'S ACRONYM(S) ARO
U.S. Army Research Office P.O. Box 12211 Research Triangle Park, NC 27709-2211	11. SPONSOR/MONITOR'S REPORT NUMBER(S) 45105-MS-MUR.83

12. DISTRIBUTION AVAILIBILITY STATEMENT

Approved for public release; Federal purpose rights

13. SUPPLEMENTARY NOTES

The views, opinions and/or findings contained in this report are those of the author(s) and should not contrued as an official Department of the Army position, policy or decision, unless so designated by other documentation.

14. ABSTRACT

We have studied the colloidal self-assembly of silica microspheres on a glass substrate patterned with triangular dimple arrays of varying pitch. Using the same silica microspheres, both charge-stabilized and hard-sphere-like binary mixtures of microspheres and nanoparticles were prepared, and their gravitational sedimentation followed by colloidal crystallization were rigorously examined in real-space using a laser scanning confocal microscopy. In wet colloidal crystals, both systems showed a strong preference toward face centered cubic (fcc) stacking, the thermodynamically stable crystal form. After drying however, only the hard-sphere-like binary mixture of silica microspheres and zirconia nanoparticle maintained the initial

15. SUBJECT TERMS

Binary mixture; Charge-stabilized; Colloidal crystal; Face centered cubic; Hard sphere; Laser scanning confocal microscopy; Triangular array

16. SECURITY CLASSIFICATION OF:			17. LIMITATION OF ABSTRACT	15. NUMBER OF PAGES	19a. NAME OF RESPONSIBLE PERSON Paul Braun
a. REPORT U	b. ABSTRACT U	c. THIS PAGE U	SAR		19b. TELEPHONE NUMBER 217-244-7293

Report Title

Epitaxially grown colloidal crystals of silica microspheres on patterned substrate of triangular arrays, Materials Science and Engineering C, 27, 961–967 (2007).

ABSTRACT

We have studied the colloidal self-assembly of silica microspheres on a glass substrate patterned with triangular dimple arrays of varying pitch. Using the same silica microspheres, both charge-stabilized and hard-sphere-like binary mixtures of microspheres and nanoparticles were prepared, and their gravitational sedimentation followed by colloidal crystallization were rigorously examined in real-space using a laser scanning confocal microscopy. In wet colloidal crystals, both systems showed a strong preference toward face centered cubic (fcc) stacking, the thermodynamically stable crystal form. After drying however, only the hard-sphere-like binary mixture of silica microspheres and zirconia nanoparticle maintained the initial templated fcc structure. The charge-stabilized system was disordered as the water was removed. Rigorous analysis of random defect structures such as stacking faults and vacancy concentration were carried out and discussed. Highly oriented colloidal crystals are of interest because of their potential use as templates for various applications.

Epitaxially grown colloidal crystals of silica microspheres on patterned substrate of triangular arrays

Wonmok Lee [1], Paul V. Braun *

Department of Materials Science and Engineering, Beckman Institute for Advanced Science and Technology, and Frederick Seitz Materials Research Laboratory, University of Illinois at Urbana-Champaign, 1304 West Green St., Urbana, IL 61801, USA

Abstract

We have studied the colloidal self-assembly of silica microspheres on a glass substrate patterned with triangular dimple arrays of varying pitch. Using the same silica microspheres, both charge-stabilized and hard-sphere-like binary mixtures of microspheres and nanoparticles were prepared, and their gravitational sedimentation followed by colloidal crystallization were rigorously examined in real-space using a laser scanning confocal microscopy. In wet colloidal crystals, both systems showed a strong preference toward face centered cubic (fcc) stacking, the thermodynamically stable crystal form. After drying however, only the hard-sphere-like binary mixture of silica microspheres and zirconia nanoparticle maintained the initial templated fcc structure. The charge-stabilized system was disordered as the water was removed. Rigorous analysis of random defect structures such as stacking faults and vacancy concentration were carried out and discussed. Highly oriented colloidal crystals are of interest because of their potential use as templates for various applications.
© 2006 Elsevier B.V. All rights reserved.

Keywords: Binary mixture; Charge-stabilized; Colloidal crystal; Face centered cubic; Hard sphere; Laser scanning confocal microscopy; Triangular array

1. Introduction

Self assembly of monodisperse colloidal microspheres into colloidal crystals is a scientifically important and technologically useful phenomenon in part because such colloidal crystals can serve as templates for 3-dimensional (3D) photonic bandgap (PBG) materials [1,2], catalysts [3], sensors [4,5] and other photonic elements [2,6,7]. Inherently, the colloidal self-assembly process results in the formation of defects which vary depending on the fabrication conditions. Random defects, including vacancies, line defects, and stacking faults, within the colloidal crystal can seriously deteriorate the performance of the final material, e.g. PBG materials [8]. To achieve low defect density single domain colloidal crystals, an understanding of the origins of such random defects is important. For a hard-sphere

system, it has been recently reported that the Gibbs-free energy difference between the face-centered cubic (fcc) and hexagonally close packed (hcp) structures is only about 10^{-4} k_BT per sphere [9,10]. Although fcc is the most stable crystal structure, colloidal crystals are usually found to be a mixture of fcc and hcp (so called random hexagonal closed packing [rhcp]) due to the small energy differences between the two structures [9]. A single hcp defect in a fcc crystal is best described as a stacking fault. The stacking fault density is lower when the colloidal crystal is formed by gravitational sedimentation as compared to formation in zero gravity [11]. Recently, van Blaaderen and coworkers rigorously investigated stacking faults in colloidal crystallization in the presence of gravitational field and topologically patterned surface. They have shown that triangular pattern arrays on the template induces a fcc colloidal crystal with a reduction in stacking fault density [12]. Along with reducing the stacking fault density, template-directed colloidal self-assembly gives control to the orientation of colloidal crystal, as first demonstrated by van Blaaderen et al. [13].

Experimentally, hard-sphere microsphere systems are formed by minimizing both van der Waals attraction and

---

electrostatic repulsion. The former can be achieved by matching refractive indices of the particle and the solvent while the latter is controlled by addition of salt [13–15]. These two requirements make it practically impossible to dry a hard-sphere system because the salt concentration changes upon drying, and generally, the solvents used to minimize the van der Waals attractions have low vapor pressures. However, for many applications, drying is essential, since otherwise the colloidal crystal can not be used as a template for other materials. We previously reported successful drying of hard-sphere-like colloidal crystals using nanoparticle mediated stabilization of silica microspheres [16]. In that system, highly charged hydrous zirconia nanoparticles promote hard-sphere-like behavior of silica spheres in acidic aqueous solution, serving to balance depletion attraction and electrostatic repulsion [17]. After colloidal crystallization is completed, the supernatant containing excess nanoparticles was carefully removed and the wet crystal was exposed to ammonia gas which lead to condensation of the zirconia nanoparticles, immobilizing the already formed silica colloidal crystal. This enabled the colloidal crystal to maintain its crystallized structure even in the presence of capillary forces exerted upon drying. This unique nanoparticle mediated stabilization and gelling coupled with template directed crystallization enabled {100} stacking of a fcc colloidal crystal with low defect densities [16].

In general, natural sedimentation without aid of a template structure on the surface prefers a triangular array since it is the most close-packed layer structure. As previously mentioned, overlying layers would find their minimum energy by fcc or hcp stacking. In this study, we rigorously examine the stacking behavior of a nanoparticle-mediated colloidal system on triangular dimple arrays throughout the fabrication sequences and compare the resulting structure with a charge-stabilized system. Real-time and real-space study of colloidal crystallization was successfully investigated by aid of laser scanning confocal microscopy (LSCM) in either reflection or fluorescence mode.

2. Experimental

2.1. Charge stabilized silica colloidal system

Uniform silica microspheres (Geltech) were purified by sedimentation and an average diameter ($d = 1.18$ µm) was determined from quantitative SEM analysis. The microspheres were first dispersed in aqueous NaCl (Aldrich) at a known concentration followed by ultrasonication (Model 550 Sonic Dismembrator, Fisher Scientific) for 1 h before sedimentation. The volume fraction of silica microspheres was fixed at 1.0×10^{-3} for all charge stabilized systems, the following NaCl concentrations were prepared: 0 M, 1 mM, 2 mM, and 10 mM. 1 mL of each suspension was added to a custom-made sample cell comprised of a glass tube (height = 2 cm, diameter = 1 cm) glued onto a flat or patterned glass cover slip which was subsequently treated with Piranha solution (sulfuric acid/hydrogen peroxide = 3:1 by volume), 1 M NaOH solution, and deionized (DI) water before each sedimentation experiment.

2.2. Binary suspension containing zirconia nanoparticle and silica microsphere

A concentrated binary suspension was prepared by the following steps. First, the same silica microspheres as used above were dispersed in DI water with volume fraction (ϕ_{micro}) 0.05. After dispersing for 18 h with magnetic stirring and three intermittent sonications during first 6 h, nitric acid (Fisher scientific) was added to adjust pH to 1.5. Then an appropriate volume fraction of hydrous zirconia nanoparticles (Zr 10/20, Nyacol Products) suspension was added to give $\phi_{nano} = 3 \times 10^{-4}$. After stirring for additional several hours, the pH of the binary suspension was readjusted to a value of 1.5. The suspension remained homogeneous and did not flocculate.

2.3. Fabrication of patterned substrate

Formation of triangular dimple arrays with various pitches were achieved by using a focused ion beam (FIB) milling system (FEI, USA). First, a glass cover slip (18 mm × 18 mm) sputter-coated with Au/Pd was fixed on FIB sample stage. A bitmap image of a triangular pattern of circles was converted to a format used by the FIB. A focused Ga ion beam (3000 pA) was scanned on the cover slip following the pattern to give 100–400 nm deep arrays of holes. The depth of holes was controlled by milling time (10–30 min) and pitch was varied by changing the magnification of the FIB system. Multiple arrays with varying depth and pitch were milled on the same cover slip. Fig. 1 shows a SEM micrograph of a patterned substrate having 400 nm depth which was milled by FIB. After patterning, the substrate was treated with aqua regia (nitric acid/hydrochloric acid = 3:1 by volume) followed by 5% HF (aq) to remove debris which formed during the FIB milling and to round the walls of the dimples, respectively. The substrate was subsequently treated
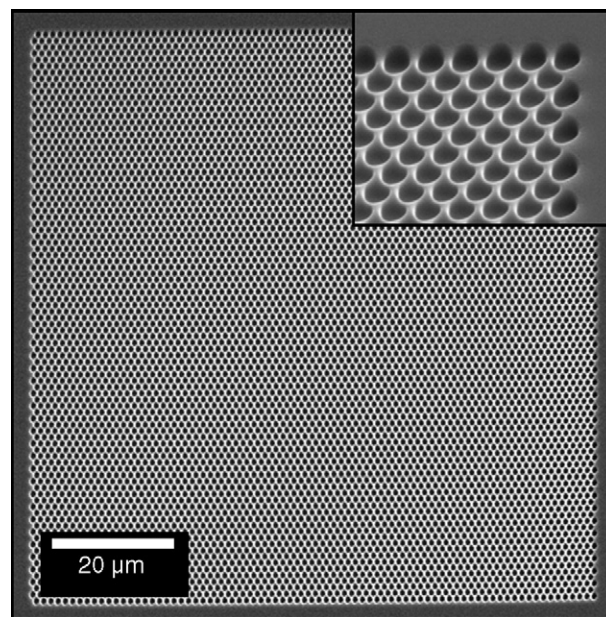

Fig. 1. SEM images of a triangular dimple array with 400 nm depth prepared by FIB milling.
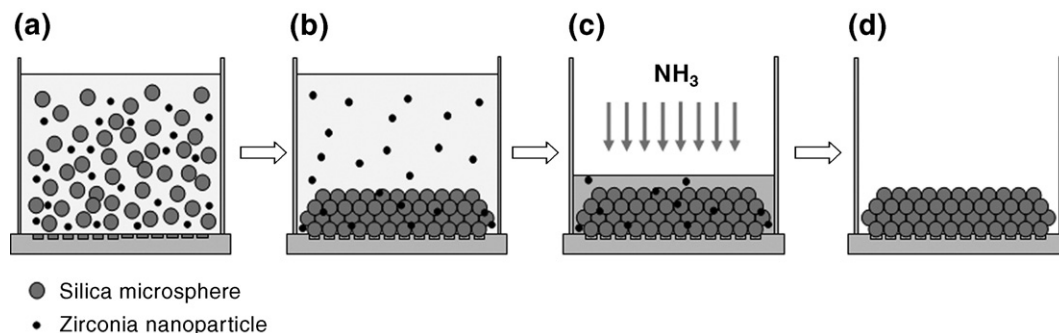
Fig. 2. Binary mixture microsphere self-assembly, gelling and drying process. (a) Binary mixture is added onto a patterned substrate, (b) gravitational sedimentation and colloidal crystallization take place, (c) supernatant is removed and ammonia vapor is introduced to induce a sol–gel transition in the zirconia nanoparticles, (d) colloidal assembly is air-dried.

with Piranha solution and then soaked in aqueous sodium hydroxide (1 M) to render the surface hydrophilic.

2.4. Sedimentation and 3D analysis of colloidal crystals by confocal microscopy

A binary fluid of colloidal silica microspheres and zirconia nanoparticles prepared as above was purified by sedimentation in a long-cylindrical glass container. An aliquot was sampled from top portion of sedimenting microspheres which corresponded to a volume fraction (ϕ_{micro}) of $\sim 10^{-3}$. Prior to addition of the purified binary fluid, a sample cell (Fig. 2(a)) was placed on the confocal microscope stage and carefully leveled. Upon introduction of 1 mL of the binary fluid (or charge-stabilized colloidal suspension), LSCM images were obtained as a function of time. The confocal microscope used in this study was Leica SP-2 equipped with an oil-immersion type objective lens (Zeiss, 63×, N.A.=1.32). During sedimentation of silica microspheres, in-situ LSCM imaging was carried out by raster-scanning 633 nm probe laser in reflection mode. Sedimentation and colloidal crystallization proceeded for 3 h. Upon completion of the crystallization, the supernatant solution was carefully removed from the sample cell and the wet colloidal sediment was exposed to ammonia vapor for 30 min

(Fig. 2(c)). During ammonia exposure, the hydrous zirconia nanoparticles gelled via condensation reactions as the pH increases from 1.5 to 9. The sample was air-dried for a day and infilled with dimethylformamide (DMF) containing Rhodamine 6G fluorescent dye (10^{-4} M) for fluorescence imaging. Since DMF is index-matched with the silica spheres, light scattering during fluorescence confocal imaging was not a problem.

3. Results and discussion

3.1. Colloidal crystallization of charge stabilized microsphere system

As microspheres sediment in under gravity field, their concentration increases and they begin to arrange themselves to a close packed structure. Generally the layer closest to the substrate adopts a close packed triangular array, and depending on colloidal system, overlying microspheres will crystallize into a rhcp structure due to very small free energy difference between fcc and hcp. Fig. 3(a) demonstrates a typical rhcp structure generated by silica microsphere of 1.18 μm diameter after gravitational sedimentation and crystallization in DI water. When silica microspheres are dispersed in pure water, the net surface charge of silica is negative due to the low pK$_a$ value of
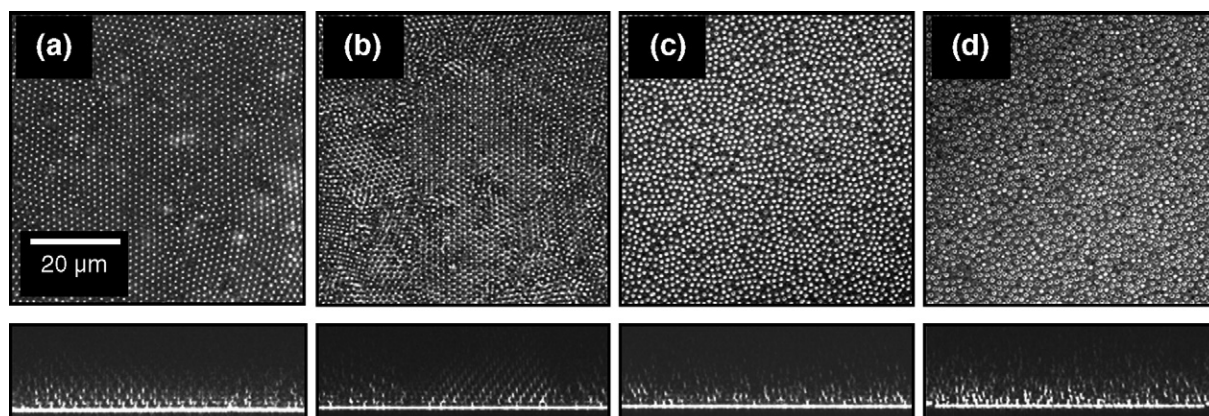

Fig. 3. Reflection mode LSCM images showing colloidal crystal formation from charge stabilized systems at varying NaCl(aq) concentrations: (a) 0 mM NaCl, (b) 1 mM NaCl, (c) 2 mM NaCl, (d) 10 mM NaCl. Upper images are of the first colloidal layer parallel to the substrate and lower images perpendicular to the substrate. Average $D_{C\text{-}C}$ of (a) and (b) are 1.38 μm and 1.27 μm, respectively. $D_{C\text{-}C}$ of (c) and (d) was not calculated due to the disorder in the first layer.

the silanol groups, and the resulting electrostatic repulsion between these like-charged particles, increases the equilibrium center-to-center distance (D_{C-C}) of the microsphere greater than the hard-sphere diameter. In the studied system, D_{C-C} was measured to be 1.38 μm. Addition of a water soluble inorganic salt, such as NaCl, decreases the Debye length (κ^{-1}) due to a screening of charge and the microspheres packing closer together. D_{C-C} for silica microspheres self-assembled in 1 mM NaCl reduces to 1.27 μm, which is still 7.6% larger than the hard-sphere diameter (1.18 μm) (Fig. 3(b)). When the NaCl concentration is increased to 2 mM, the microspheres aggregate and do not crystallize because the screened coulombic repulsion is not sufficient to overcome van der Waals attractions. Some locally crystalline regions are found at 2 mM NaCl, but generally a colloidal glass is formed. At 10 mM NaCl a completely random colloidal structure is found. The van der Waals attraction can be eliminated by the use of a solvent system, which has the same refractive index as the colloidal microspheres. For silica microsphere, previous studies have employed mixtures of dimethylformamide (DMF) and dimethylsulfoxide (DMSO), or a mixture of glycerol and water [12,13]. However, a critical shortcoming of those mixtures are their low volatility, which makes drying difficult. We have excluded the use of non-volatile solvents because our applications require a dry colloidal crystal.

Wet colloidal crystals from the charge-stabilized system (NaCl 1 mM) tended toward fcc rather than rhcp as shown in *xz*-image of Fig. 3(b). It was previously reported that fcc is the stable structure for colloidal systems with long-ranged repulsive interactions at high volume fractions [18,19]. Also, the presence of gravitational forces perpendicular to the bottom-wall has been reported to lead colloidal systems to prefer fcc [12]. This same microsphere suspension (1 mM NaCl) was settled on a patterned surface consisting of shallow dimples (depth= 100 nm) on a 1.28 μm pitch. This pitch is just slightly larger than the average D_{C-C} of the microspheres (1.27 μm) when sedimented on a flat surface. Colloidal crystals sedimented from 1 mM NaCl onto the triangular pattern preferred fcc similar to a flat surface and the orientation of the crystals was clearly determined by the surface topology, indicating suc-

cessful colloidal epitaxy. Fig. 4(a) and (b) present the bottom layer of the charge-stabilized colloidal self-assembly before and after solvent drying, respectively. In both images, the microspheres on the flat surface and patterned surface can be seen simultaneously due to a shallow depth of the pattern. Upon drying, most of the particles adjacent to the flat substrate move significantly due to changes in salt concentration and capillary forces upon drying. However, colloidal particles sitting on the dimple array did not leave their initial position. This is probably due to a combination of the increased van der Waals attraction between the rounded dimple and the overlying silica microsphere, and the fact that capillary forces will tend to pull the particle into the dimple in the final stages of drying. On a flat substrate, neither of these mechanisms operates. This effect however does not hold for microspheres in upper layers. In Fig. 5 (a) and (c), a bottom layer *xy*-image and a cross-section *xz*-image of dried and dye-backfilled colloidal assembly from the same sample (charge-stabilized system) is shown in fluorescence mode. Despite the perfect triangular array of silica microspheres in the bottom layer, upper layers have completely disordered upon drying.

3.2. Colloidal crystallization of hard-sphere-like binary nanoparticle microsphere system

The binary nanoparticle microsphere system contains the same microspheres as used for the charge-stabilized colloidal system, however the behavior is dramatically different due to the addition of nanoparticles, including hard-sphere-like behavior near the silica isoelectric point (pH ~2.5) [17]. In our previous investigation, we demonstrated that {100} stacking of the silica microsphere on square array of holes resulted in a nearly perfect epitaxially grown 3-D fcc crystal which maintained its structures throughout the drying process [16]. Because the crystal was grown via {100} stacking the resulting crystal could be formed to be free of stacking faults or line defects. It however was not clear as to what the result would be if the colloidal crystal was epitaxially grown on a triangular array of holes, which is the focus of the present study. In this case, the
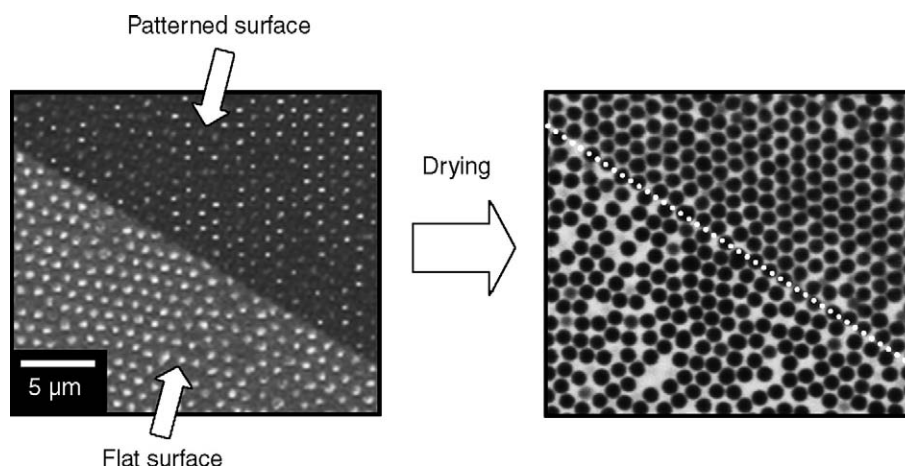

Fig. 4. LSCM images of bottom layer colloidal self-assembly settled from charge-stabilized (NaCl 1 mM) silica microsphere solution: (a) Reflection mode image before drying, (b) fluorescence mode image after drying and dye back-filling.
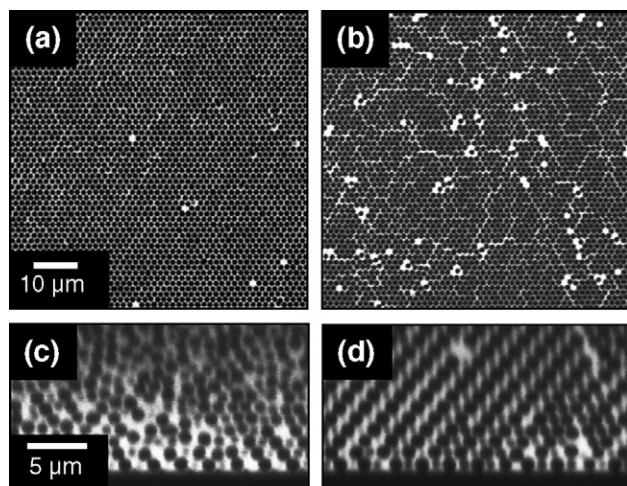
Fig. 5. Fluorescence LSCM images of dried microspheres self-assembled on the 100 nm deep triangular dimple array prepared by various routes. (a, c) From a charge-stabilized (NaCl 1 mM) silica microsphere solution; (b, d) from a binary mixture of the silica microspheres and zirconia nanoparticles. (a) and (b) are images of the bottom layer of each system and (c) and (d) are cross-sectional image of (a) and (b) taken at the middle of each image. Both dried colloidal crystals were dye back-filled prior to imaging.

resulting colloidal crystal is expected to be similar to that formed on a flat surface (e.g. {111} fcc planar to bottom surface), however it was not clear how the presence of the topological restriction of the substrate would impact the orientation of the bottom and the overlying layers. Fig. 5(b,d) presents fluorescence LSCM images of a final dried colloidal crystal created from a binary mixture settled on a triangular patterns similar to that shown in Fig. 1. The pitch was 1.21 μm, copying the pitch found in our previous study [16] to be optimal for this binary system. D_{C-C} of silica microspheres is 1.20 μm under the conditions of the studies.

It is worth noting that the vacancy concentration on the first layer is much larger in a binary system than in a charge-stabilized system. This is most likely because the hard-sphere system is much less tolerant of microsphere polydispersity. Because the pitch in the binary system is almost the same as the microsphere diameter, even slightly larger than average particles will not fit into the bottom layer. The charge-stabilized

system is much 'softer', and thus more tolerant of microsphere polydispersity. We previously observed that the vacancy concentration is strongly modulated by the pitch, and increases as pitch decreases [16]. The crystal structure is surprisingly perfect other than the vacancy concentration in the first layer. As presented in Fig. 5(d), cross-sectional image of a colloidal crystal formed from the binary suspension is surprisingly fcc and contains very few stacking faults. Following is a more rigorous discussion of these issues.

Fig. 6 shows time-dependent cross-sectional LSCM images of colloidal crystal formation from binary suspension on a deep (400 nm) dimple array throughout the crystallization process. Ten minutes after addition of colloidal suspension revealed the first (bottom) layer has not crystallized. After 20 min crystallization has clearly started and reaches completion by 180 min and the crystal is clearly apparent (Fig. 6(c)). The crystal exhibits nearly perfect ABC stacking (fcc). Upon removal of the majority of the supernatant, the lowest three layers rearranged perhaps due to an inadvertent shearing, which means that a perturbation in bulk liquid transmitted a shear force to the bottom layers exceeding energy barrier for rearrangement. The crystalline structure was however maintained during gelation and drying, indicating no further rearrangements during these processing steps, as expected. Because the structure is not changed by gelling and drying, the complete 3D structure can be determined by backfilling the dried colloidal crystal with an index matched solvent containing a fluorescent dye (fluorescence imaging is much more quantitative than reflection imaging, which often contains artifacts).

A similar experiment was then carried, except on a shallow (100 nm) dimple array (Fig. 7). Here, the fcc wet crystal did not rearrange upon supernatant removal (Fig. 7b) perhaps because a shear force has been dissipated at the shallow dimples which perhaps allowed the movement of the bottom layer particles while deep dimples did not, or perhaps the shear force upon drying of this sample was less. The gelled and dried colloidal crystal also maintained a nearly perfect fcc structure as shown by a fluorescence LSCM image of dye-backfilled crystal (Fig. 7(d)).

The dimensionless Peclet number, $Pe = 4/3\pi\Delta\rho g R^4 kT^{-1}$, the gravitational energy relative to the thermal energy of a colloidal system, is a parameter to measure the tendency for colloidal
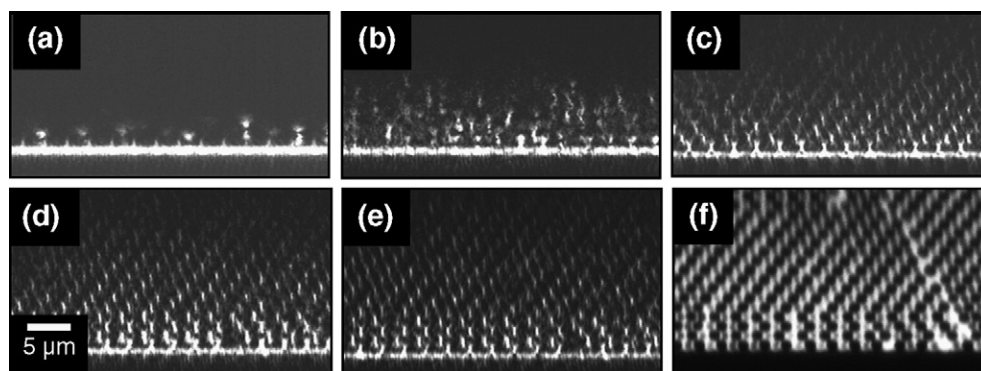

Fig. 6. Cross-sectional LSCM images showing sedimentation and colloidal crystallization on a 400 nm deep triangular dimple arrays taken (a) 10 min, (b) 30 min, (c) 180 min after addition of binary mixture. Other images are taken (d) after supernatant removal, (e) after ammonia exposure, (f) after air-drying and dye back-filling.
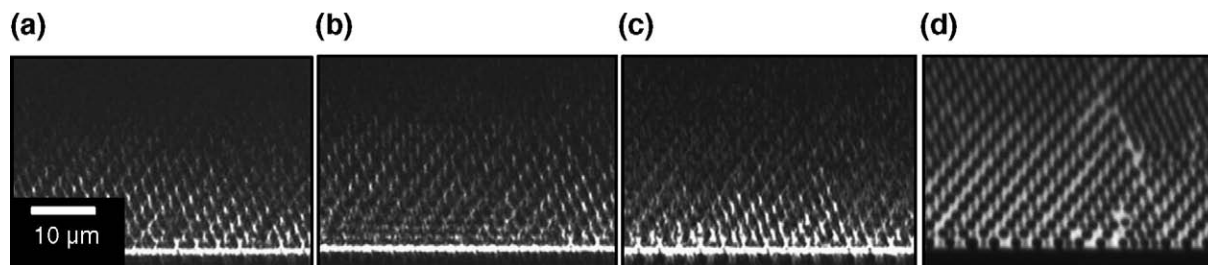
Fig. 7. Cross-sectional LSCM images showing sedimentation and colloidal crystallization on a shallow (100 nm deep) triangular dimple arrays taken (a) 180 min after addition of binary mixture. Other images are taken (b) after supernatant removal, (c) after ammonia exposure, (d) after air-drying and dye back-filling.

crystallization. Pe of our system is calculated to be 1.5, which is an order of magnitude larger than that of the hard-sphere systems employed in the previous study [12]. Increased gravitational energy is considered to have influenced stacking sequence to prefer fcc stacking as predicted by van Blaaderen and co-workers [12].

We examined the pitch size effect on stacking faults and vacancy concentration in the overlying colloidal crystals. The stacking parameter (α) of a fcc crystal domain is given as the following [20],

$$\alpha = 1 - \kappa/(N-2)$$

and it can be measured by counting number of kinks (κ) at each layer number (N) from a LSCM image of {110} plane [12]. In {110} plane, fcc stacking can be distinguished by ABC stacking of the layers. If there is no kink, the crystal is a pure fcc ($\alpha = 1$) while a pure rhcp gives α equals to 0.5. $\langle \alpha \rangle$ of 20 layers was measured for the colloidal crystals grown on three triangular arrays having pitches of 1.19 μm, 1.21 μm and 1.23 μm, respectively. The depth of pattern was 100 nm for every case. Observed stacking parameters are summarized in Table 1 where a variation of ~3% in pitch size does not have a significant effect on stacking parameter. However, stacking faults were found to be concentrated at lower layers (i.e. <4th layer). There might be several reasons for the location of stacking faults at lower layers. As mentioned before, there is a supernatant re-moval step in our process which always has a risk to exert a shear force to perturb the already formed colloidal crystal. In the patterned region, the bottom crystalline layer is rather strongly bound to the dimple arrays, while the upper layers are of course not bound to the substrate, so a shear force could induce a rearrangement. van Blaaderen and coworkers have reported a higher density of stacking faults in the lower layers of colloidal crystals and they ascribed this to a kinetic factor, results from a

low crystallization rate in the bottom three layers due to high osmotic pressure [12]. However, average stacking parameters above the 4th layer were calculated to be greater than 0.93 regardless of substrate pitch. The stacking parameter of the colloidal crystals formed on flat substrates also had a strong preference towards fcc with overall $\langle \alpha \rangle$ even greater than the crystals formed on the patterned substrate. However, these crystals also contained grains as small as 30 μm across which tend towards rhcp.

Unlike the pitch independent stacking faults density, the vacancy concentration in the bottom layer was significantly affected by pitch as plotted in Fig. 8. As the pitch decreased from 1.21 μm to 1.19 μm, only a 1.7% change, the number of vacancies doubled. As the pitch approaches the colloidal diameter, it becomes increasingly difficult to fill every dimple, perhaps because diffusion slows down as the volume fraction of the colloids locally increases, or due to larger particles which do not fit into the pattern. The vacancy concentration above the 3rd layer was almost independent of pitch size as shown in Fig. 8, perhaps indicating that packing at the substrate interface is more difficult than onto a layer of colloids. We previously observed that epitaxially grown colloidal crystals on square array patterns show a strong pitch effect in vacancy concentration even in upper layers. In that work, as the pitch increases, the number of vacancies was reduced. Although it is not clear, perhaps the greater stability of the {111} crystallographic plane as compared to the {100} plane decreases vacancy density.
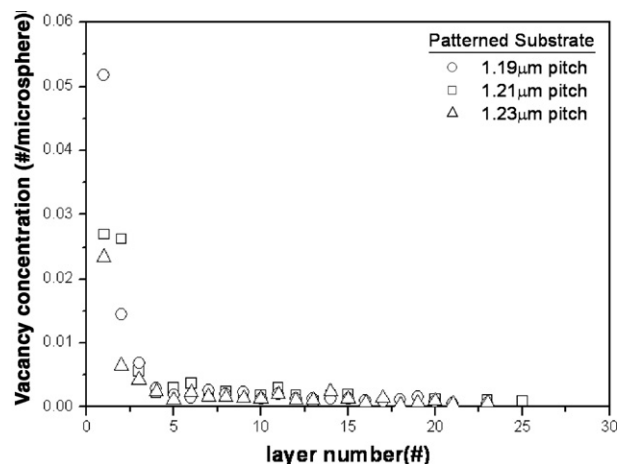
Table 1
Average stacking parameters of the colloidal crystals grown on the patterned substrate with varying pitch

Pitch	$\langle \alpha \rangle$	$\langle \alpha \rangle_{L>4}$
1.19 μm	0.86 ± 0.18	0.96 ± 0.06
1.21 μm	0.81 ± 0.14	0.93 ± 0.11
1.23 μm	0.84 ± 0.18	0.93 ± 0.10

Each value was averaged up to the 20th layer. $\langle \alpha \rangle_{L>4}$ denotes the stacking parameter averaged from 4th to 20th layer.

Fig. 8. Vacancy concentration of a colloidal crystal vs. layer number grown on a patterned substrate as a function of the pitch.

4. Conclusion

We have demonstrated template-assisted colloidal crystallization of the silica microspheres from a charge-stabilized system and a nanoparticle-mediated hard-sphere-like system. The use of a LSCM enabled real-time, real-space investigations of colloidal crystallization onto patterned substrate. Although the charge-stabilized system preferred fcc stacking in wet crystal, those crystalline structures were completely disordered during solvent removal due to an abrupt change of salt concentration and capillary forces. Taking advantage of the sol–gel transition of zirconia-nanoparticle upon a pH change, dried colloidal crystals from binary mixtures were obtained in which more than 90% of crystal was fcc and oriented with respect to the pattern on the substrate containing the triangular hole array.

Acknowledgments

References

[1] P.W. Anderson, Phys. Rev. 109 (1958) 1492.
[2] J.D. Joannopoulos, R.D. Meade, J.N. Winn, Photonic Crystals: Molding the Flow of Light, Princeton University Press, N.J., 1995.
[3] B.T. Bolland, C.F. Blanford, Science 281 (1998) 538.
[4] J.H. Holtz, S.A. Asher, Nature 389 (1997) 829.
[5] Y.J. Lee, P.V. Braun, Adv. Mater. 15 (2003) 563.
[6] S. John, Phys. Rev. Lett. 58 (1987) 2486.
[7] G. Pan, R. Kesavamoorthy, S.A. Asher, Phys. Rev. Lett. 78 (1997) 3860.
[8] Y.A. Vlasov, V.N. Astratov, A.V. Baryshev, A.A. Kaplyanskii, O.Z. Karimov, M.F. Limonov, Phys. Rev., E 61 (2000) 5784.
[9] S. Pronk, D. Frenkel, J. Chem. Phys. 110 (1999) 4589.
[10] L.V. Woodcock, Nature 385 (1997) 141.
[11] J.X. Zhu, M. Li, R. Rogers, W. Meyer, R.H. Ottewil, W.B. Russel, P.M. Chaikin, Nature 387 (1997).
[12] J.P. Hoogenboom, D. Derks, P. Vergeer, A. van Blaaderen, J. Chem. Phys. 117 (2002) 11320.
[13] A. van Blaaderen, R. Ruel, P. Wiltzius, Nature 385 (1997) 321.
[14] P.V. Braun, R.W. Zehner, C.A. White, M.K. Weldon, C. Kloc, S.S. Patel, P. Wiltzius, Adv. Mater. 13 (2001) 721.
[15] A.D. Dinsmore, A.G. Yodh, D.J. Pine, Nature 383 (1996) 239.
[16] W. Lee, A. Chan, M.A. Bevan, J.A. Lewis, P.V. Braun, Langmuir 20 (2004) 5262.
[17] V. Tohver, J.E. Smay, A. Braem, P.V. Braun, J.A. Lewis, Proc. Natl. Acad. Sci. U. S. A. 98 (2001) 8950.
[18] E.B. Sirota, H.D. Ou-Yang, S.K. Sinha, P.M. Chaikin, J.D. Axe, Y. Fujii, Phys. Rev. Lett. 62 (1989) 1524.
[19] F. El Azhar, M. Baus, J.P. Ryekaert, E.J. Meijer, J. Chem. Phys. 112 (2000) 5121.
[20] M.S. Elliot, T.F. Bristol, W.C.K. Poon, Physica, A 235 (1997) 216.